IOP PUBLISHING JOURNAL OF PHYSICS: CONDENSED MATTER

J. Phys.: Condens. Matter **19** (2007) 145202 (9pp) doi:10.1088/0953-8984/19/14/145202

Detecting spontaneous symmetry breaking in finite-size spectra of frustrated quantum antiferromagnets

Grégoire Misguich[1] **and Philippe Sindzingre**[2]

[1] Service de Physique Théorique, URA CNRS 2306, CEA Saclay, 91191 Gif sur Yvette, France
[2] Laboratoire de Physique Théorique de la Matière Condensée, Université P et M Curie, 75252 Paris Cedex, France

Received 19 September 2006
Published 23 March 2007
Online at stacks.iop.org/JPhysCM/19/145202

Abstract

Exact diagonalization is a powerful numerical technique for analysing static and dynamical quantities in quantum many-body lattice models. It provides unbiased information concerning quantum numbers, energies and wavefunctions of the low-energy eigenstates for almost any kind of microscopic model. The information about energies and quantum numbers is particularly useful to detect possible spontaneous symmetry breaking at $T = 0$. We review some of the advances in the field of frustrated quantum magnets which have been possible thanks to detailed symmetry analysis of exact diagonalization spectra. New results concerning the kagome and star lattice Heisenberg antiferromagnets are presented.

1. Introduction

There exists a wide range of numerical techniques to deal with quantum many-body problems. In the field of lattice spin Hamiltonians, the quantum Monte Carlo and density matrix renormalization group (DMRG) techniques are among the most powerful, in particular because they allow one to study very large systems accurately. None of them is, however, efficient for studying *frustrated* models in dimensions $D > 1$. These systems, in $D = 2$ in particular, can present a large variety of phases, with potentially new exotic phases of matter [1].

Although limited to small system sizes, exact diagonalizations (EDs) give very valuable information on these frustrated systems. They can provide (almost) any physical quantity: energies, gap, quantum numbers, static and dynamical correlations, thermodynamics, ... The method has *no bias*, and requires no particular knowledge of the low-energy physics. It has been applied from the beginning of numerical investigations of quantum spin models.[3]

The first question to address in order to characterize a state of matter concerns the (spontaneously) broken symmetry(ies). A natural way to do so is to evaluate possible order parameters from appropriate correlation functions in systems of increasing sizes and study if

[3] In 1964, Bonner and Fisher [2] studied an 11-site spin-$\frac{1}{2}$ chain by ED.

they might remain finite in the thermodynamic limit. Thanks to the rapid growth of computing power, the available system sizes have increased a lot since the first ED studies.[4] Still, these sizes (a few tens of sites at most) are sometimes too small to decide if a given order parameter vanishes in the infinite size limit. In these cases an approach based on *spectrum analysis* can be very useful to detect broken symmetries. It is simply based on the fact that a spontaneous symmetry breaking (SSB) at $T = 0$ implies some ground-state (quasi-)degeneracy on finite-size spectra. This paper illustrates the power of this method through a few examples and references to recent studies of 2D quantum antiferromagnets. Some new data on the spin-$\frac{1}{2}$ Heisenberg model on the kagome and 'expanded-kagome' lattices (EKLs) will also be presented.

2. Basics of the exact diagonalization method

This section is a brief presentation of the ED method. It is intended for the non-specialist and is not specific to studies of frustrated magnets. Some readers may therefore wish to go directly to section 3.

2.1. Lanczos method

The Lanczos method is a numerical iterative algorithm especially efficient at finding a few extremal eigenvalues and eigenstates (at both ends of the spectrum) for a big sparse Hermitian matrix. Starting from an initial random vector, one iteratively builds an orthonormal basis of the Hilbert space in which the Hamiltonian is tri-diagonal. The spectrum of the growing tri-diagonal matrix progressively converges to the spectrum of the Hamiltonian. The power of the method comes from the fact that the *extremal* eigenvalues converge first. In particular, the lowest eigenvalue of the tri-diagonal matrix converges (exponentially fast) to the true ground-state energy. The number of iterations required to obtain the ground state with a good accuracy is *much* smaller than the Hilbert space dimension. In a typical case, the two first eigenvalues of a matrix of size 10^6 are obtained with machine accuracy in about only 100 iterations (matrix–vector multiplications). Once the ground state has been found, a variant of the Lanczos algorithm may be used to compute dynamical correlations (for a recent example, see [5]) or the spin-stiffness [6].

2.2. Other algorithms—full diagonalization

Standard algorithms/libraries (like LAPACK) allow one to obtain the *full* spectrum of a Hermitian matrix. The available Hilbert space dimensions are then however much smaller (typically a few 10^4 for a few gigabytes of memory) than with the Lanczos method. Full diagonalization allows one to compute the finite-temperature properties of the system exactly. This may also be a step in solving a generalized diagonalization eigenvalue problem such as arises when the microscopic spin model has been projected onto a variational subspace in a non-orthogonal basis, such as the subspace of first-neighbour valence bond coverings (see [7, 8] and section 3.4 below for an example).

2.3. Symmetries

The ED method becomes really powerful only when the spectrum is computed separately in each symmetry sector. The symmetry analysis can be described mathematically on general

[4] In [3] the ground state of a 40-site spin-$\frac{1}{2}$ model was computed. A star lattice with 42 sites was studied in [4].

grounds. One first determines the symmetry group $\mathcal{G}$ of the Hamiltonian $\hat{\mathcal{H}}$ and[5] the irreducible representations (IRs) $\gamma_0, \gamma_1, \ldots, \gamma_n$ of $\mathcal{G}$. The projector $\hat{\Pi}_\alpha$ onto the subspace which transforms according to γ_α (symmetry sector α) reads $\hat{\Pi}_\alpha = \frac{1}{|\mathcal{G}|}\sum_{g\in\mathcal{G}} \chi_\alpha(g)\hat{g}^{-1}$, where $\chi_\alpha(g) = \mathrm{Tr}[\gamma_\alpha(g)]$ is the character of γ_α for the group element g (denoted $\hat{g}$ when acting on physical states). By construction, the $\hat{\Pi}_\alpha$ are orthogonal and commute with $\hat{\mathcal{H}}$. Thus one can diagonalize $\hat{\mathcal{H}}$ separately in the image of each projector (symmetry sectors). In fact, one can further refine the decomposition of the Hilbert space. For a given sector α, $\hat{\Pi}_\alpha$ can be written as a sum: $\hat{\Pi}_\alpha = \sum_{i=1}^{d_\alpha} \hat{\pi}_\alpha^i$. d_α is the dimension of the IR γ_α, the $\hat{\pi}_\alpha^i$ are defined by $\hat{\pi}_\alpha^i = \frac{1}{|\mathcal{G}|}\sum_{g\in\mathcal{G}} \gamma_\alpha^{(i,i)}(g)\hat{g}^{-1}$ and $\gamma_\alpha^{(i,i)}(g)$ is the ith diagonal element of $\gamma_\alpha(g)$ (in some arbitrary basis). The $\hat{\pi}_\alpha^i$ also form a family of orthogonal projectors commuting with $\hat{\mathcal{H}}$. The spectrum need not be computed for all subspaces $\mathrm{Im}[\hat{\pi}_\alpha^i]$. One spectrum (e.g. $i = 1$) will be enough since, in sector α, all the $\hat{\pi}_\alpha^{i=1,\ldots,d_\alpha}$ give the same eigenvalues (hence a degeneracy equal to the IR dimension d_α).

Such a symmetry analysis offers many advantages. The decomposition into stable orthogonal subspaces allows one to work with smaller vectors and requires less memory and CPU time. The density of states being much smaller in each sector than in the full spectrum, convergence is reached faster. In the subspace $\mathrm{Im}[\hat{\pi}_\alpha^{i=1}]$, the eigenvalues are (generically) *non-degenerate*. The actual degeneracy of an energy level (hard to find with the Lanczos technique if symmetries were not used) is simply given by the IR dimension d_α. The knowledge of the IRs of each energy level is very important in detecting SSB.

In many cases the IRs of the full lattice symmetry group can be obtained from *one-dimensional* representations of some subgroups (the IRs are *induced* by some subgroup representations). In practice, this amounts first to fixing the lattice momentum k and then looking for IRs of its *little group* (which leaves k invariant). Such a simplified description in terms of one-dimensional representations of a subgroup is however not always possible (examples: symmetry group of the icosahedron [9]).

2.3.1. Implementations. Usually, a full projection in individual symmetry sectors of $SU(2)$ with total spin S is not implemented. This requires large extra CPU time/memory and is not necessary. Instead, one merely uses a $U(1)$ subgroup, which is a conservation of S^z_{total} with spin-flip symmetry in the sector $S^z_{\mathrm{total}} = 0$ which projects on the subspaces with S even or odd. For $SU(2)$ invariant Hamiltonians, an energy level of spin S will then be degenerate in sectors $|S^z| \leqslant S$ which allows one to infer the value of S. As regards lattice symmetries, a fully automatic treatment can be implemented. As an example, the spectra shown in section 3.4 were obtained by a program with automatic detection of lattice symmetries and construction of the corresponding IRs (using GAP [10]) and application of the appropriate projectors π. However, to our knowledge, no software with such an systematic/automatic treatment of lattice symmetries is publicly available at present.

3. Detecting spontaneous symmetry breaking

3.1. Quantum numbers

The existence of an SSB (at $T = 0$) in the thermodynamic limit has direct consequences on the structure of the low-energy spectrum (degeneracies, quantum numbers). Although the SSB

[5] In the case of a Heisenberg model on a 2D finite lattice with periodic boundary conditions, this group is the direct product of $SU(2)$ (global spin rotations) and the lattice symmetry group. The latter usually contains translations as well as point group symmetries (lattice rotations and axis reflections).

only takes place in the thermodynamic limit, this structure is often visible on (very) small systems, provided the that the model is not too close to a (quantum) phase transition. It is a very useful signature of SSB in ED studies.

The basic idea is the following. Let $|\psi\rangle$ be a ground state of the system and $\mathcal{G}$ the symmetry group of the Hamiltonian. If $|\psi\rangle$ is a *broken symmetry state*, there exists, by definition, at least one group element $g \in \mathcal{G}$ under which $|\psi\rangle$ is not invariant: $|\langle\psi|\hat{g}|\psi\rangle| < 1$. The linear space $V_{\rm gs}$ generated by all the states $\{\hat{g}|\psi\rangle, g \in \mathcal{G}\}$ has thus a dimension $d > 1$; it defines a (non-trivial) linear representation Γ of $\mathcal{G}$. Because any $g \in \mathcal{G}$ commutes with the Hamiltonian, all the states of $V_{\rm gs}$ are degenerate ground states. The decomposition of Γ onto IRs γ_α of $\mathcal{G}$: $\Gamma = \bigoplus_\alpha n_\alpha \gamma_\alpha$ is obtainable from group theory. One finds that the spectrum contains exactly n_α ground state(s) in the symmetry sector labelled by the IR α (for $n_\alpha \neq 0$). The multiplicities n_α may be obtained from the following character representation formula:

$$n_\alpha = \frac{1}{|\mathcal{G}|} \sum_{g\in\mathcal{G}} \chi_\alpha(g^{-1}) \sum_{|i\rangle} \langle i|\hat{g}|i\rangle \tag{1}$$

where the states $|i\rangle$ form an orthonormal basis of the ground-state manifold $V_{\rm gs}$. This can also be written as $n_\alpha = \sum_i ||\hat{\Pi}_\alpha|i\rangle||^2$, so that $n_\alpha > 0$ if and only if a broken symmetry state has a non-zero projection on sector α. Of course, these multiplicities *only* depend on the symmetry properties of $V_{\rm gs}$. They can therefore be computed by choosing a simpler state, $|\psi_0\rangle$ (without quantum fluctuations for instance), belonging to the same 'phase'. At this stage the problem of finding the n_α has been reduced to a purely group-theoretical problem[6]. If the system has a finite size, the different sectors with $n_\alpha > 0$ will not be exactly degenerate. Still, for a large enough system they should become the lowest eigenstates of the spectrum.

3.2. Discrete broken symmetry, valence-bond crystals

For a discrete broken symmetry, there are a finite number of degenerate ground states in the thermodynamic limit, separated by a gap (finite in the thermodynamic limit) from physical excitations. This (quasi-)degeneracy does not depend on the system size (provided boundary conditions do not frustrate the order). In frustrated magnets, valence-bond crystals (VBCs) are the simplest examples [1]. The procedure described in section 3.1 gives a straightforward relation between the VBC pattern and the quantum numbers of the quasi-degenerate ground-states. For a large enough system, one can therefore directly read off the spatial symmetries of the possible VBC from the spectrum, without computing any correlation function. To confirm the SSB in the thermodynamic limit, one eventually has to check the exponential decay of the energy splitting between the quasi-degenerate ground-states. A complementary method based on reduced density matrices [11] can then be used to determine 'automatically' the order parameter and the VBC pattern.

Recent ED studies have exhibited various VBC phases. Some 2D examples for $SU(2)$ symmetric spin-$\frac{1}{2}$ models are on the honeycomb [12] and square lattices [13, 14, 3, 15]. The case of the kagome antiferromagnet will be discussed from a VBC point of view in section 3.5 and a new example on the EKL in section 3.4. VBC orders may occur in more complex models, but ED remain there, limited to quite small sizes. For example, ED studies of a 2D $SU(4)$ spin–orbital model on the square lattice indicate the possibility of a VBC phase there [16].

[6] This is particularly simple for one-dimensional representations. In that case one first determines the subgroup H of symmetry operations which leaves all the broken symmetry states invariant. Only the sectors where $\chi_\alpha(h) = 1$ for *all* $h \in H$ can have $n_\alpha > 0$.

3.3. Broken continuous symmetry: Néel and nematic phases

The structure of the spectrum is richer for *continuous* broken symmetries than for discrete ones. First, the existence of gapless Goldstone modes makes the distinction between 'ground states' and 'excitations' more subtle. And since the ground-state subspace ($V_{\rm gs}$) has a infinite dimension in the thermodynamic limit (one can perform infinitesimal rotations of the initial broken symmetry state), the number of quasi-degenerate ground states has to grow as a function of the system size.

Frustrated magnets exhibit a remarkably large variety of phases with broken continuous symmetries. In a Néel phase, the lattice spontaneously breaks up into sublattices in which the all spins point in the same direction (up to quantum zero-point fluctuations). The simplest example is the two-sublattice collinear structure realized (at $T = 0$) in the (unfrustrated) antiferromagnetic Heisenberg model on the square lattice. But frustration can lead to much more complex structures with non-collinear [17, 3] and non-coplanar [18] sublattice magnetizations, order-by-disorder effects [19], nematic phases with broken $SU(2)$ symmetry but no sublattice magnetization [3, 20], etc.

To obtain the quantum numbers of the finite-size ground states in Néel systems, one has to decompose a broken-symmetry Néel state $|\psi_0\rangle$ (with a well-defined direction for the sublattice magnetizations) onto the IR of the $SU(2)$ and lattice symmetry groups. As explained above, we can consider a 'classical' Néel state with maximum sublattice magnetization (each sublattice is fully polarized). For the two-sublattice problem $|\psi_0\rangle$ can be chosen as an Ising state $|\psi_0\rangle = |\uparrow\downarrow\uparrow\downarrow\cdots\rangle$. Although trivial, the two-site case is instructing: $|\psi_0\rangle = |\uparrow\downarrow\rangle \sim |S = 0\rangle + |S = 1, S^z = 0\rangle$ is the linear combination of a singlet state *and* a triplet ($S = 1$) state. Similarly, a general classical Néel state for N (even) sites will have a finite overlap on *all total spin sectors* from $S = 0$ to $S = N/2$. Still, the weight of the different spin sectors decreases with increasing S in a Néel state (which has no net magnetization in any direction) and one has in particular $\langle\psi_0|\vec{S}^2_{\rm total} = S(S+1)|\psi_0\rangle \sim N$. From this we can guess that, in fact, only spin sectors from $S = 0$ to $S \sim \sqrt{N}$ are required to construct a state with finite (but not maximum) sublattice magnetization and non-zero quantum fluctuations. A simple semiclassical argument allows one to guess the finite-size scaling of the energies for these states (the so-called 'Anderson tower' [21], or QDJS in [17, 22]). As for classical spins, one expects a finite uniform susceptibility per site χ in a quantum Néel phase. The total magnetization M is therefore given by $\simeq N\chi B$ in the presence of an (infinitesimal) applied field B. M is also obtained by minimizing $E(M) - M\cdot B$, where $E(M)$ is the energy of the lowest state with total spin $S = M$ (in zero field). Combining the two leads to $E(S) = S^2/(2N\chi)$. This spectrum of the Anderson tower corresponds physically to the (slow) quantum dynamics of the 'rigid body' made by the macroscopic ($\sim N$) sublattice magnetizations; it should not be confused with physical spin-wave excitations (higher in the spectrum). As expected, the states with $S \lesssim \sqrt{N}$ collapse onto the ground state (up to a total energy $\mathcal{O}(1)$) in the $N \to \infty$ limit so that a broken symmetry state (some combinations of the QDJS) has an energy per site $\epsilon \sim 1/N \to 0$. This structure (including space group quantum numbers, not discussed here) involves many ($\sim\sqrt{N}$) states and imposes strong constraints on the low-energy spectrum. It has been observed numerically in finite-size spectra for a large number of quantum antiferromagnets (see [22] and references therein). This tower structure offers a very efficient way to recognize systems with continuous broken symmetries, as it already shows up on very small systems (the energy gaps in the Anderson tower ($\sim 1/N$) decay more quickly than the finite-size corrections to the sublattice magnetization ($\sim 1/\sqrt{N}$)). Collinear versus non-collinear Néel states can also be readily discriminated from their spectra. A collinear structure has a tower with exactly *one* level per value of S whereas the tower of a non-collinear system (with $\geqslant 3$ sublattices) contains

$2S + 1$ levels in the total spin sector S. We also mention that tower structures have also been discussed (and observed numerically) for larger symmetry group, like $SU(4)$, in the context of spin–orbital models [23].

A similar analysis can be carried out for quantum p (resp. n) spin-nematics [24], which are systems with broken $SU(2)$ symmetry but no sublattice magnetization. A simple picture is that the spins spontaneously select a preferred oriented (resp. non-oriented) *plane*, but no particular *direction* (the order parameter is an antisymmetric (resp. symmetric) rank-2 tensor in the spin variables). Again, such a broken symmetry state is a linear combination of many finite-size eigenstates of the systems, with specific (and predictable by group theory) total spin and spatial quantum numbers. As examples, we mention two recent ED studies which exhibited the tower structures associated to a 2D p- [3] and n- [20] nematics.

3.4. $J_e - J_t$ model on the expanded kagome lattice

The EKL (also dubbed star lattice [4]) is obtained from the kagome lattice by splitting each site into two, and inserting an 'expanded' bond connecting the two neighbouring triangles. Its plaquettes are triangles and dodecagons and all the sites are equivalent. Concerning frustration, the classical antiferromagnetic Heisenberg model on the EKL has a huge degeneracy equivalent to that on the kagome lattice [4]. Since the EKL has two kinds of bond (triangle and 'expanded' bonds), it is natural to consider a $J_t - J_e$ spin-$\frac{1}{2}$ Heisenberg model (both antiferromagnetic here). To our knowledge this model has only been studied for $J_e = J_t$ so far [4].

The limit $J_e \gg J_t$ is simple: the system is made of weakly coupled *bonds*, the ground state is unique (spin singlet) and all excitations are gapped ($\Delta \sim J_e$); it is an *explicit VBC* (terminology of [1]) without any broken symmetry. The model has been shown [4] to be in this phase at least up to $J_t/J_e = 1$.

The limit of weakly coupled triangles ($J_e \ll J_t$) is more interesting as the ground state is extensively degenerate at $J_e = 0$ (four degenerate ground states per triangle). As in Mila's work on the trimerized kagome lattice [25], the degenerate perturbation theory for $J_e/J_t \ll 1$ can be formulated as a spin-chirality Hamiltonian. In fact, Mila's self-consistent mean-field solution of this Hamiltonian almost directly applies on the EKL. As a result, one finds an *extensive* number of (mean-field) ground states which are in one-to-one correspondence with some particular singlet coverings of the EKL (dubbed 'super coverings' hereafter). These singlet coverings are those which maximize the number of occupied J_t bonds (as expected since $J_t \gg J_e$). But the extensive degeneracy is clearly an artefact of the mean-field approximation.

To go beyond, we performed some ED of the EKL Heisenberg model *restricted the subspace of first-neighbour valence bond coverings* (a method initiated for the kagome antiferromagnet [7]). As a justification, we note that this variational RVB subspace contains both the exact $J_t = 0$ ground state (a singlet on each J_e bond) as well as all the mean-field solutions (super coverings) of $J_e/J_t \ll 1$. The subspace dimension is $2^{(N+1)}$ for N dodecagons and periodic boundary conditions[7], which is much smaller than total Hilbert space dimension 2^{6N}. Because different singlet coverings are not orthogonal, the matrices are not sparse and we had to resort to full diagonalizations. Using all lattice symmetries, the complete spectrum has been obtained for $N = 12$ and 16 and a part of the spectrum for $N = 18$.[8] The results are summarized in figure 1. The spectrum evolves from a regime with one ground state and a large gap ($J_t/J_e \lesssim 1.1$) to a regime with many low-energy states ($J_t/J_e \gtrsim 1.3$). As expected,

[7] As for the kagome lattice [7, 26], there is a mapping between dimer coverings and Ising pseudo-spin configurations.

[8] The two four-dimensional IRs (subspace dimensions $> 29 \times 10^3$) corresponding to the eight wavevectors indicated by three-leg symbols in the Brillouin zone (right of figure 1) could *not* be computed for $N = 18$ (108 sites) because of memory limitations.

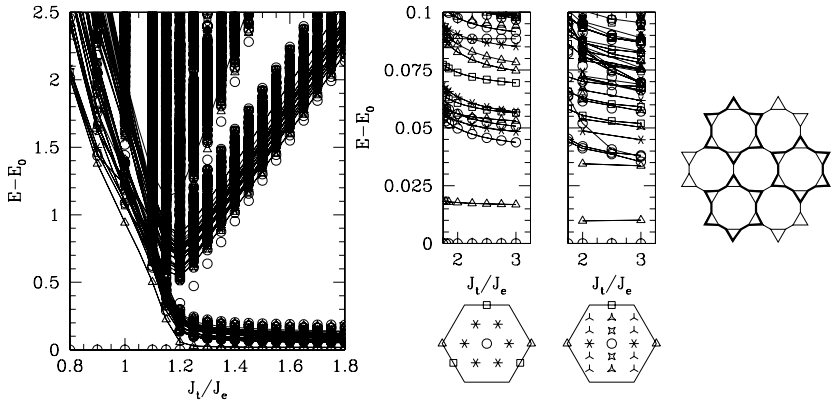

Figure 1. Spectrum of the $J_e - J_t$ spin-$\frac{1}{2}$ Heisenberg Hamiltonian (on the EKL) projected in the first-neighbour RVB subspace. Left and middle spectra: lattice with 12 dodecagons (72 sites). Right spectrum: 18 dodecagons (108 sites). The wavevector symbols are indicated below, in the corresponding Brillouin zones. The VBC pattern proposed for $J_t \gtrsim 1.3 J_e$ is shown on the right of the figure (the singlet 'stars', with 18 sites, are marked with fat bonds).

the number of such low-energy states matches the number of super coverings. For $J_t/J_e \gtrsim 1.3$ one energy level, corresponding to an IR of dimension 2 and momentum in the zone corner, is significantly below the other excited states (and goes further down from $N = 12$ (middle spectrum) to $N = 18$ (right spectrum)). This is what one expects for an SSB towards a three-fold degenerate VBC. From the momenta ($k = (0, 0)$ and $k = (0, \pm 4\pi/3)$), such VBC should be invariant under any three-step translations and the simplest guess is a crystal with resonating 'stars' (an analogue to that found in the hexagonal lattice quantum dimer model [27]), as shown at the right of figure 1. This is also natural because the energy gained by singlet resonances is larger with small loops, and the 18-site stars are the shortest loops made out (three) super dimers. Although further investigations are certainly needed to confirm the existence of this VBC, the spectra (in this variational approximation) clearly show that it is the most likely scenario.

3.5. Antiferromagnetic spin-$\frac{1}{2}$ Heisenberg model on the kagome lattice

It has been argued that the kagome antiferromagnet could form a VBC at *very* low energies. One scenario [28, 7, 29] is a crystal (VBC-1 in the following), which maximizes the number of 'perfect' hexagons in a way which preserves the $2\pi/3$ rotation symmetry of the lattice (see figure 2 of [29]). Using the method of section 3.1, we computed the quantum numbers associated to this crystal for a 36-site sample[9]. The lowest exact eigenstates (obtained by ED [30]) matching these quantum numbers are marked by $*$ in column VBC-1 of table 1. Although one cannot exclude a deep reorganization of the low-energy levels when increasing the system size, these states are *not* the lowest ones. Similarly, a four-fold degenerate crystal of resonating 12-site 'stars' [31] would require the two levels indicated in column VBC-2 to become the lowest states. The quantum numbers of the 'columnar' VBC proposed in [32] (degeneracy 24) correspond to the last column (VBC-3). In all cases, the crystallization would require a complete reshuffling of the low-energy spectrum.

[9] The quantum numbers σ and R_2 may depend on the relative sign of the two singlet coverings participating in a plaquette resonance (here, hexagons and stars). These signs were determined by minimizing the energy (by ED) in a variational a subspace of first-neighbour singlet coverings.

Table 1. Low-energy levels of the Heisenberg model on a 36-site kagome lattice (all are total spin singlets) [30]. Momentum $k = A$ refers to the three middle points of the (hexagonal) zone boundary, B to the two corners of the Brillouin zone. The six points C correspond to $\pm B/2$. R_3 (resp. R_2) indicates (when applicable) the phase factor acquired by the wavefunctions under a $2\pi/3$ (resp. π) rotation around the centre of a hexagon. σ is the parity under reflection about the momentum direction. For $k = 0$, the reflection axis σ is chosen parallel to a lattice bond. The eigenstates whose quantum numbers match those of VBC ground states (see text) are marked by $*$ in the last columns.

Number	$2\langle\vec{S}_i \cdot \vec{S}_j\rangle$	k	R_3	R_2	σ	Deg.	VBC-1	VBC-2	VBC-3
1	−0.438 376 53	0	1	1	1	1		*	*
2	−0.438 095 62	B	$e^{\pm 2i\pi/3}$			4			
3	−0.438 070 91	0	$e^{\pm 2i\pi/3}$	1		2			*
4	−0.437 993 46	0	1	1	1	1			
5	−0.437 851 05	C			1	6			
6	−0.437 585 10	0	1	−1	1	1			*
7	−0.437 584 55	A		1	1	3	*		*
8	−0.437 519 41	C			−1	6	*		
9	−0.437 215 66	0	1	1	−1	1	*		*
10	−0.437 187 96	0	$e^{\pm 2i\pi/3}$	1		2			*
11	−0.437 147 65	A		−1	−1	3			*
12	−0.437 051 08	0	$e^{\pm 2i\pi/3}$	−1		2			*
13	−0.437 039 81	B	1		1	2	*		
14	−0.437 034 69	A		−1	1	3			*
15	−0.436 858 67	0	1	−1	−1	1			*
16	−0.436 853 19	B	1		−1	2			
17	−0.436 837 57	A		1	−1	3		*	*
...	...	...		...		...			
44	−0.434 745 19	0	$e^{\pm 2i\pi/3}$	−1		2			*

Acknowledgments

We are grateful to A Läuchli, C Lhuillier and L Pierre for many discussions and collaborations on these topics and to J Schulenburg for correspondence about the software Spinpack.

References

[1] Misguich G and Lhuillier C 2005 *Frustrated Spin Systems* ed H T Diep (Singapore: World-Scientific) (Review chapter) (*Preprint* cond-mat/0310405)
[2] Bonner C and Fisher M E 1964 *Phys. Rev.* **135** 640
[3] Läuchli A, Domenge J C, Lhuillier C, Sindzingre P and Troyer M 2005 *Phys. Rev. Lett.* **95** 137206
[4] Richter J, Schulenburg J, Honecker A and Schmalfuß D 2004 *Phys. Rev.* B **70** 174454
[5] Läuchli A and Poilblanc D 2004 *Phys. Rev. Lett.* **92** 236404
[6] Einarsson T and Schulz H J 1995 *Phys. Rev.* B **51** 6151
[7] Zeng C and Elser V 1995 *Phys. Rev.* B **51** 8318
[8] Mambrini M and Mila F 2000 *Eur. Phys. J.* B **17** 651
[9] Pierre L 2006 private communication
[10] The GAP Group—*Groups, Algorithms, and Programming* package GRAPE (www.gap-system.org)
[11] Furukawa S, Misguich G and Oshikawa M 2006 *Phys. Rev. Lett.* **96** 047211
[12] Fouet J B, Sindzingre P and Lhuillier C 2001 *Eur. Phys. J.* B **20** 241
[13] Läuchli A, Wessel S and Sigrist M 2002 *Phys. Rev.* B **66** 014401
[14] Fouet J B, Mambrini M, Sindzingre P and Lhuillier C 2003 *Phys. Rev.* B **67** 054411
[15] Mambrini M, Läuchli A, Poilblanc D and Mila F 2006 *Preprint* cond-mat/0606776

[16] Van den Bossche M, Zhang F C and Mila F 2000 *Eur. Phys. J.* B **17** 367
[17] Bernu B *et al* 1992 *Phys. Rev. Lett.* **69** 2590
Bernu B *et al* 1994 *Phys. Rev.* B **50** 10048
[18] Domenge J C, Sindzingre P, Lhuillier C and Pierre L 2005 *Phys. Rev.* B **72** 024433
[19] Lecheminant P, Bernu B, Lhuillier C and Pierre L 1995 *Phys. Rev.* B **52** 6647
[20] Shannon N, Momoi T and Sindzingre P 2006 *Phys. Rev. Lett.* **96** 027213
[21] Anderson P W 1952 *Phys. Rev.* **86** 694
[22] Lhuillier C 2005 *Preprint* cond-mat/0502464
[23] Penc K, Mambrini M, Fazekas P and Mila F 2003 *Phys. Rev.* B **68** 012408
[24] Andreev A F and Grishchuk I A 1984 *Sov. Phys.—JETP* **60** 267
[25] Mila F 1998 *Phys. Rev. Lett.* **81** 2356
[26] Misguich G, Serban F and Pasquier V 2002 *Phys. Rev. Lett.* **89** 137202
[27] Moessner R, Sondhi S L and Chandra P 2001 *Phys. Rev.* B **64** 144416
[28] Marston J B and Zeng C 1991 *J. Appl. Phys.* **69** 5962
[29] Nikolic P and Senthil T 2003 *Phys. Rev.* B **68** 214415
[30] Waldtmann C *et al* 1998 *Eur. Phys. J.* B **2** 501
Waldtmann C 2000 *PhD Thesis* Universität Hannover
[31] Syromyatnikov A V and Maleyev S V 2002 *Phys. Rev.* B **66** 132408
[32] Budnik R and Auerbach A 2004 *Phys. Rev. Lett.* **93** 187205